

## The *Icsbp* locus is a common proviral insertion site in mature B-cell lymphomas/plasmacytomas induced by exogenous murine leukemia virus

Shi Liang Ma<sup>a</sup>, Annette Balle Sørensen<sup>a</sup>, Sandra Kunder<sup>b</sup>, Karina Dalsgaard Sørensen<sup>a</sup>, Leticia Quintanilla-Martinez<sup>b</sup>, David W. Morris<sup>c,1</sup>, Jörg Schmidt<sup>d</sup>, Finn Skou Pedersen<sup>a,\*</sup>

<sup>a</sup> Department of Molecular Biology, University of Aarhus, C.F. Møllers Alle, Bldg. 130, DK-8000 Aarhus C, Denmark

<sup>b</sup> Institute of Pathology, GSF-National Research Center for Environment and Health, D-85764 Neuherberg, Germany

<sup>c</sup> Sagres Discovery, Davis, CA 95617, USA

<sup>d</sup> Department of Comparative Medicine, GSF-National Research Center for Environment and Health, D-85764 Neuherberg, Germany

Received 20 January 2006; returned to author for revision 16 February 2006; accepted 3 May 2006

Available online 15 June 2006

### Abstract

ICSBP (interferon consensus sequence binding protein)/IRF8 (interferon regulatory factor 8) is an interferon gamma-inducible transcription factor expressed predominantly in hematopoietic cells, and down-regulation of this factor has been observed in chronic myelogenous leukemia and acute myeloid leukemia in man. By screening about 1200 murine leukemia virus (MLV)-induced lymphomas, we found proviral insertions at the *Icsbp* locus in 14 tumors, 13 of which were mature B-cell lymphomas or plasmacytomas. Only one was a T-cell lymphoma, although such tumors constituted about half of the samples screened. This indicates that the *Icsbp* locus can play a specific role in the development of mature B-lineage malignancies. Two proviral insertions in the last *Icsbp* exon were found to act by a poly(A)-insertion mechanism. The remaining insertions were found within or outside *Icsbp*. Since our results showed expression of *Icsbp* RNA and protein in all end-stage tumor samples, a simple tumor suppressor function of ICSBP is not likely. Interestingly, proviral insertions at *Icsbp* have not been reported from previous extensive screenings of mature B-cell lymphomas induced by endogenous MLVs. We propose that ICSBP might be involved in an early modulation of an immune response to exogenous MLVs that might also play a role in proliferation of the mature B-cell lymphomas.

© 2006 Elsevier Inc. All rights reserved.

**Keywords:** Murine leukemia virus; Insertional mutagenesis; B-cell lymphomas; Plasmacytoma; Common integration site

### Introduction

Interferon (IFN) consensus sequence binding protein (ICSBP), also known as interferon regulatory factor 8 (IRF8), is a member of a family of transcription factors termed IFN regulatory factors (IRFs) (Driggers et al., 1990; Taniguchi et al., 2001). It is a 50 kDa protein first identified as an interferon  $\gamma$  (IFN $\gamma$ ) inducible protein that binds to the promoter of the MHC class 1 gene through the interferon consensus sequence (ICS). Originally identified as a transcription repressor (Weisz et al., 1992), ICSBP regulates transcription in the immune system (Tamura and Ozato, 2002; Wang et al., 2000) through multiple target DNA elements, including IFN-stimulated response

element (ISRE) (Darnell et al., 1994; Harada et al., 1989; Kessler et al., 1988; Tanaka et al., 1993), Ets/IRF composite element EICE (Driggers et al., 1990; Eisenbeis et al., 1995; Klemsz et al., 1990; Marecki et al., 2001; Rao et al., 1999), IFN-gamma activation site (GAS) (Contursi et al., 2000; Darnell et al., 1994), and hematopoiesis-associated factor-1(HAF1)-*cis* element (Kakar et al., 2005). The DNA-binding motif of ICSBP shares significant sequence similarities with other IRF family members at the first 115 amino acids, which comprise the DNA-binding domain (DBD) (Sharf et al., 1995). ICSBP exerts its transcriptional activity through interaction with other IRF members, by protein–protein interaction through the IRF association domain (IAD) (Levi et al., 2002) that, except for IRF1 and IRF2, shares sequence similarities among the IRF members. In addition, ICSBP interacts with other transcription factors, such as PU1, E47, and NFAT, through the PEST domain (Bovolenta et al., 1994; Eklund and Kakar, 1999; Meraro et al.,

\* Corresponding author. Fax: +45 8619 6500.

E-mail address: [fsp@mb.au.dk](mailto:fsp@mb.au.dk) (F.S. Pedersen).

<sup>1</sup> Current address: OncoNex Corporation, Davis, CA 95617, USA.

1999). The dual role of ICSBP is demonstrated by the fact that interaction with IRF-1 or IRF-2 on ISRE leads to the formation of a heterocomplex with repression activity, while on the contrary, interactions with PU.1 and E47, or NFAT result in the formation of transcriptional activation heterocomplexes (Rehli et al., 2000; Schmidt et al., 2004; Zhu et al., 2003).

Among the IRFs, ICSBP is expressed exclusively in cells of the immune system such as monocytes/macrophages, dendritic cells, B-cells, and activated T-cells (Driggers et al., 1992; Lu et al., 2003; Nelson et al., 1993; Schiavoni et al., 2002; Tsujimura et al., 2002; Weisz et al., 1994; Weisz et al., 1992). A number of studies have established an essential role for ICSBP in the differentiation of myeloid progenitor cells toward mature macrophages while blocking differentiation toward granulocytes (Tamura et al., 2000; Tamura and Ozato, 2002), and it has been shown that mice with *Icsbp* null mutation are defective in this feature (Wang et al., 2000). In fact, several studies have confirmed that ICSBP does play a role in regulating pathways affecting myeloid lineage commitment (Nagamura-Inoue et al., 2001), including a study in which lineage marker-negative (Lin<sup>-</sup>) bone marrow progenitor cells were used to validate the involvement of ICSBP in controlling myeloid lineage proliferation. It was shown that an ICSBP-deficient mouse developed granulocytic leukemia, a condition very similar to human chronic myelogenous leukemia (CML) (Holtzschke et al., 1996). In line with this, low levels of *Icsbp* transcripts have been observed in human acute myeloid leukemia (AML) and CML patients, where the decreased transcript levels could be reversed by treatment with IFN- $\alpha$  (Schmidt et al., 1998). In other studies, a significantly decreased ICSBP expression level was observed in BCR-ABL-induced CML disease, and by using a mouse model, it was shown that forced co-expression of ICSBP attenuated BCR-ABL induced CML (Hao and Ren, 2000). In contrast to a well-documented role in the myeloid lineage, reports of the role of the *Icsbp* gene in B-cell or T-cell development are quite sparse. Still, one study showed B-cell development blockage in *IRF4*<sup>-/-</sup>, *ICSBP*<sup>-/-</sup> mice, without impairing T-cell development in the thymus (Lu et al., 2003), and very recently Lee et al. (2006) have shown by siRNA knockdowns of ICSBP expression in a mouse B-cell lymphoma cell line that activation-induced cytidine deaminase (AID) and BCL6 might be important transcriptional targets of ICSBP.

Retroviral insertional mutagenesis has been studied in different mouse models (Hansen et al., 2000; Jonkers and Berns, 1996; Martin-Hernandez et al., 2001), and with complete mouse genome information available, proviral tagging has become a powerful tool for the identification of cancer-related genes (Kim et al., 2003; Mikkers et al., 2002a, 2002b; Suzuki et al., 2002). In that respect and to broaden our understanding of diseases in the hematopoietic system, we have used the inbred NMRI mouse strain infected with the nonacutely transforming, ecotropic murine leukemia viruses (MLVs), Akv and SL3-3 retroviruses, as prototypic models of B- and T-cell tumorigenesis, respectively.

By means of high-throughput screening procedures, we here report of the finding of 14 MLV proviral insertions at

the *Icsbp* locus, 13 of which are from the B-lymphotropic Akv (or derivatives thereof)-induced lymphomas, while a single one is from a diffuse large B-cell lymphoma induced by an SL3-3 variant containing severe enhancer mutations. Remarkably, we did not observe any hits in SL3-3 MLV-induced T-cell lymphomas, which led us to examine possible, specific functions of *Icsbp* expression in MLV-induced B-cell lymphomas. Overall, our findings strongly suggest a differential role of *Icsbp* in B-cell lymphomagenesis as compared to T-cell lymphomagenesis. However, as no major changes of *Icsbp* RNA or protein expression levels in the end-stage tumor samples could be observed, a straightforward oncogenic overexpression or tumor suppressor function of *Icsbp* in B-cell tumors is unlikely.

## Results

### *The Icsbp locus is a frequent target in MLV-induced lymphomas*

Screening tumors from 1203 mice resulted in about 3000 retroviral tags. Of these, 14 integrations (from 14 different mice) were found within a 100 kb region encompassing the *Icsbp* locus, which is 140 times higher than the average frequency of 3000 integrations over the whole genome. The tagging-site selection difference from randomness was supported statistically by applying the ( $\chi^2$ ) test ( $P < 0001$ ). This strongly indicates that the *Icsbp* insertions have been selected for during lymphomagenesis and hence that *Icsbp* can indeed play a role in lymphoma development.

As seen in Fig. 1, the integration sites were evenly distributed along the *Icsbp* locus without any orientation preference. Nine integrations were found in the same, and 5 in the opposite transcriptional orientation as compared to that of the target gene.

### *Icsbp integrations are specific for tumors of B-cell origin*

Since about half of the investigated tumors resulted from experimental series employing viruses belonging to the T-lymphomagenic SL3-3 MLV type (Table 1), it is striking that all but one of the *Icsbp* integrated proviruses were found in tumors induced by the Akv MLV type, and moreover, the single one not conforming to this type was found in a tumor induced by a seriously weakened enhancer mutant of SL3-3. Mutants from this series did not at all behave like the conventional SL3-3 MLV type, i.e. they did not induce T-cell lymphomas, and indeed histopathology analyses of this particular tumor revealed that it could be classified as a diffuse large B-cell lymphoma (Table 2).

By morphological examination, all 14 mice in question presented with enlargement of spleen and mesenteric lymph nodes, and in two cases a slightly enlarged thymus was observed as well. This is in contrast to what is usually observed for SL3-3 MLV-infected mice, which in almost 100% of the cases display a significant thymus enlargement.

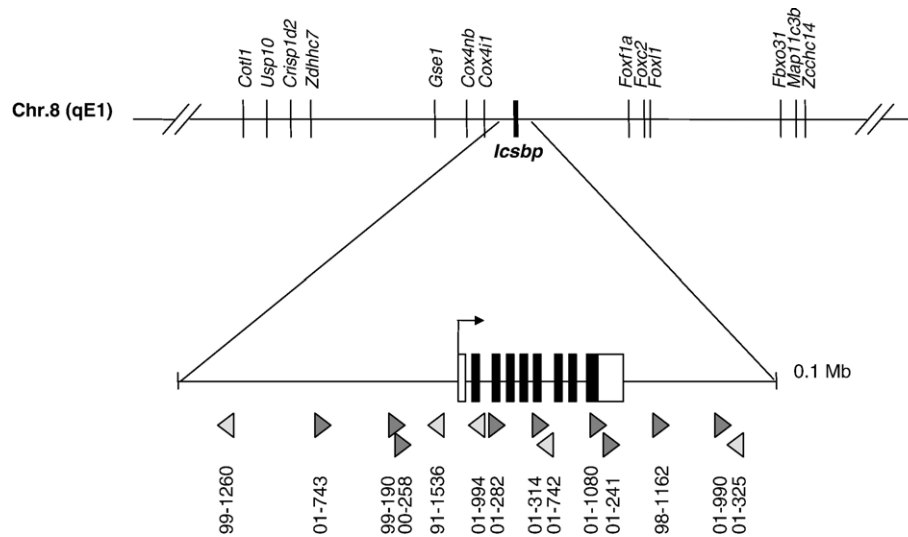


Fig. 1. The *Icsbp* locus and inserted proviruses. Upper panel: map of the *Icsbp* locus and flanking genes on mouse chromosome 8. The distance between *Icsbp* and *Cox4i1* is 37.832 bp, and between *Icsbp* and *Foxf1a* is 325.958 bp (UCSC assembly; mm6). Lower panel: exon–intron map of the *Icsbp* transcription unit with indication of positions and transcriptional orientations of inserted proviruses in tumor DNAs marked by tumor IDs. A total of 14 proviral insertions within a  $1 \times 10^5$  bp window at the *Icsbp* locus are depicted, 5 upstream of, 6 within, and 3 downstream of the predicted *Icsbp* transcription unit. The triangles indicate the transcription orientation of the proviruses. The nine *Icsbp* exons are marked as rectangles with the coding regions in black and the noncoding regions in white. Exon 9 harbors coding sequences followed by a long 3'-untranslated region.

Of the 14 *Icsbp* integrations, 12 were found in DNA from enlarged spleens, while 2 were identified in DNA of enlarged thymuses (99-190 and 98-1162).

Southern blotting analyses (summarized in Table 2) with TCR- $\beta$  probes did not, except in a single case (which also revealed rearrangements of *Ig $\kappa$*  and *IgH*), show rearrangements of the TCR- $\beta$  gene in any of the examined tumor samples (data not shown), indicating that the *Icsbp*-targeted lymphomas are not in general of T-cell origin. This was further supported by the observations of frequent rearrangements of *Ig $\kappa$*  and/or *IgH* genes, when the same Southern membranes were hybridized with probes recognizing these genes (data not shown); accordingly, these results pointed to a B-cell tumor phenotype of the *Icsbp* tumors. Finally, hybridizations with *Icsbp* cDNA and ecotropic-specific envelope probes did not reveal any clonal provirus integrations (examples are provided in Fig. 2), which – with respect to provirus integration – indicate tumors of a polyclonal nature.

Table 1  
Distribution of *Icsbp* locus integrations among virus/host models

Model, virus type <sup>a</sup> /mouse strain <sup>b</sup>	No. of mice tagged (no. of mice with <i>Icsbp</i> integrations)
Akv/NMRI-i	524 (13)
Akv/SWR	37 (0)
SL3-3/NMRI-r	58 (1)
SL3-3/NMRI-i	327 (0)
SL3-3/SWR	98 (0)
Akv + SL3-3/NMRI-i	159 (0)
Total	1203 (14)

<sup>a</sup> Virus type indicates wild type as well as all derived mutants.

<sup>b</sup> NMRI-i denotes inbred NMRI; NMRI-r, randomly bred NMRI.

#### *Tumors with Icsbp insertions are mostly diffuse large B-cell lymphomas and plasmacytomas*

As summarized in Table 2, the hematopoietic neoplasms observed in the lymphoid organs of 14 mice infected with viruses with proviral insertion sites at the *Icsbp* locus could be classified as plasmacytoma (PCT) (6/14; 43%), diffuse large B-cell lymphoma (DLBCL) (6/14; 43%), or precursor T-cell lymphoblastic lymphoma (pre-T LBL) (1/14; 7%). In only one case (1/14; 7%; tumor 01-743), no histological evidence for a neoplastic disease, but a reactive plasma cell proliferation was found. In this case, a moderate proliferation of plasma cells and hyperplastic reactive germinal centers were observed.

Peripheral lymph nodes and the spleen were enlarged in all animals. In plasmacytomas, in addition to a severe plasma cell proliferation, which destroyed the normal architecture of the lymph nodes (Fig. 3G), hyperplastic germinal centers without a mantle zone, so called “naked germinal centers”, were observed. In the spleen, both the red and the white pulp were affected, and also nonlymphoid organs, e.g. liver, were massively infiltrated by neoplastic plasma cells (Fig. 3H). Plasma cells were either medium-sized (Figs. 3G–I) with a monotonous morphology or slightly pleomorphic with bigger, irregular-shaped nuclei, and a blastic chromatin pattern (Figs. 3J–L). Plasma cells were CD79acy-positive and CD138-positive or -negative. It should be noted that a remaining normal hematopoiesis was still present in all mice.

The infiltration pattern of diffuse large B-cell lymphomas in the spleen and lymph nodes was diffuse (Figs. 3D–F) and large neoplastic B-cells were B220- and CD79acy-positive (not shown) with abundant pale cytoplasm, big nuclei with open chromatin, and one to three distinct nucleoli. Many mitotic figures indicated a high proliferation rate, which was also

Table 2  
Tumor panels of mice harboring integrations in the *Icsbp* locus

Tumor ID	Virus variant <sup>a</sup>	Mouse strain	Lymphoma incidence, n/total	Mean latency, days (SD)	Specific tumor latency, days	Tumor phenotype				Histopathology <sup>c</sup>
						DNA analysis <sup>b</sup>				
						Igκ	IgH	TCR	Eco	
01-282	Akv wt	NMRI-i	16/16	178 (31)	181	+	+	+	P	DLBCL
98-1162	Akv wt	NMRI-i	20/20	161 (36)	140	–	–	–	P	DLBCL
99-190	Akv PBS lys	NMRI-i	20/20	206 (30)	225	–	–	–	P	DLBCL
01-241	Akv1-99 wt	NMRI-i	18/19	179 (18)	175	+	+	–	P	DLBCL
01-325	Akv1-99 wt	NMRI-i	16/16	179 (18)	173	–	–	–	P	PCT
00-258	Akv SA' gag mutant (CD)	NMRI-i	17/20	209 (26)	245	ND	ND	ND	ND	PCT
01-994	Akv1-99 mEa/s	NMRI-i	42/42	163 (23)	170	+	–	–	P	PCT
01-1080	Akv1-99 mEa/s	NMRI-i	5/5	182 (9)	183	–	–	–	P	PCT
01-314	Akv1-99 (mEgre + mEa/s)	NMRI-i	44/44	154 (44)	106	ND	ND	ND	ND	pre-T LBL
01-990	Akv1-99 (mEgre + mEa/s)	NMRI-i	44/44	154 (44)	231	ND	ND	ND	ND	PCT
01-742	Akv1-99 (mRunx I + mEgre)	NMRI-i	27/28	204 (27)	183	+	–	+	P	PCT
01-743	Akv1-99 (mRunx I + mEgre)	NMRI-i	27/28	204 (27)	183	–	–	–	P	Plasma cell proliferation
99-1260	Akv1-99 (dm NF1)	NMRI-i	18/20	186 (26)	225	–	+	–	P	DLBCL
91-1536	SL3-3 Runx dm	NMRI-r	1/19	NA	190	ND	ND	ND	ND	DLBCL

NA indicates not applicable; and ND, not determined.

<sup>a</sup> The viruses mentioned here originated from published work (Ethelberg et al., 1997, 1999; Hallberg et al., 1991; Lovmand et al., 1990, 1998; Lund et al., 1999; Olsen et al., 1990; Sorensen et al., 2005) as well as unpublished pathogenicity studies.

<sup>b</sup> The tumor DNA was analyzed by Southern blot hybridizations using probes detecting rearrangements in Igκ, IgH, or TCR (+ denotes rearrangement; – denotes no rearrangement). An ecotropic specific probe (Eco) was used to detect clonally integrated proviruses; P denotes a polyclonal-like pattern, i.e. many weak (or no) hybridizing fragments.

<sup>c</sup> Histological and immunohistological analyses were performed as described. DLBCL denotes diffuse large B-cell lymphoma; PCT, plasmacytoma; and pre-T LBL, precursor T-cell lymphoblastic lymphoma.

demonstrated with anti Ki-67 immunohistochemistry (Fig. 3E), and many reactive CD3-positive T-cells were present (Fig. 3F). In addition, reactive eosinophilic granulocytes and histiocytes were intermingled with the neoplastic cells.

One tumor was classified as a precursor T-cell lymphoblastic lymphoma (Figs. 3A–C). Thymus, spleen, cervical, and mesenteric lymph nodes were enlarged. At lower magnification, a distinct starry sky pattern with many tingible bodies was present, especially in the thymus. Monotonous, blastic, medium-sized, CD3-, and TdT-positive tumor cells (Figs. 3B, C) showed a high proliferation rate and were infiltrating lymphatic and nonlymphatic tissues. This T-cell tumor developed with a slightly shorter latency period (106 days) as compared to the other tumors. In this exceptional case, both spleen, from which the *Icsbp* integration was found, and thymus were analyzed, and both tissues exposed the same phenotype. In spite of the single exceptional case, which may or may not represent a random integration (i.e. an integration not selected for during tumor development), the overall picture remains that *Icsbp* insertions are tightly associated with mature B-cell neoplasms.

#### No major effect of proviral insertions on *Icsbp* mRNA levels

In order to analyze a possible effect of the *Icsbp* integrated proviruses on the *Icsbp* mRNA pattern in the MLV-induced tumors, Northern blot analyses were performed for 10 of the 14 tumors, in which both a change in the amount of mRNA and a change in transcript sizes were detected. Four different *Icsbp* cDNA probes (depicted in Fig. 4), covering different parts of the cDNA, were generated.

In order to distinguish a change in mRNA pattern likely to be caused by an integrated provirus, mRNA from tumors from the same experimental series – but without an integration in the *Icsbp* locus – served as controls. These control tumors thus exemplify the typical *Icsbp* mRNA pattern in an MLV-induced tumor. Examples of Northern blot analyses of different experimental series are shown in Figs. 4, 5, and 6. These show that the general *Icsbp* expression pattern in the MLV-induced tumors consists of two transcripts of 3.0 kb and 1.7 kb, respectively, a pattern which is in agreement with published results for the mouse *Icsbp* gene (Driggers et al., 1990). Probe 537 (exon 2 to exon 5) as well as probe 841 (exon 5 to exon 9) detected both transcripts, whereas probe 909 (representing just exon 9) detected only the larger 3.0 kb transcript (Fig. 4). When probe 47-1270 (covering all the coding sequences from exon 2 to 9) was used, again both transcripts were detected (Fig. 4), suggesting that the two transcripts share the same coding sequence, and that the shorter transcript most likely is generated by use of the alternative polyadenylation signal in exon 9 (indicated in Fig. 4).

The two transcripts of 3.0 and 1.7 kb were seen in all cases irrespective of the presence or absence of provirus integrations into the *Icsbp* locus (Fig. 4), and, with the exception of the formation of chimeric transcripts (Figs. 5 and 6, discussed later), no major changes in expression levels were observed. Accordingly, provirus insertion into the *Icsbp* locus does not in general seem to affect the *Icsbp* mRNA pattern in MLV-induced end-stage tumor tissues. This implies that neither a straightforward overexpression of an oncogene nor an extinction

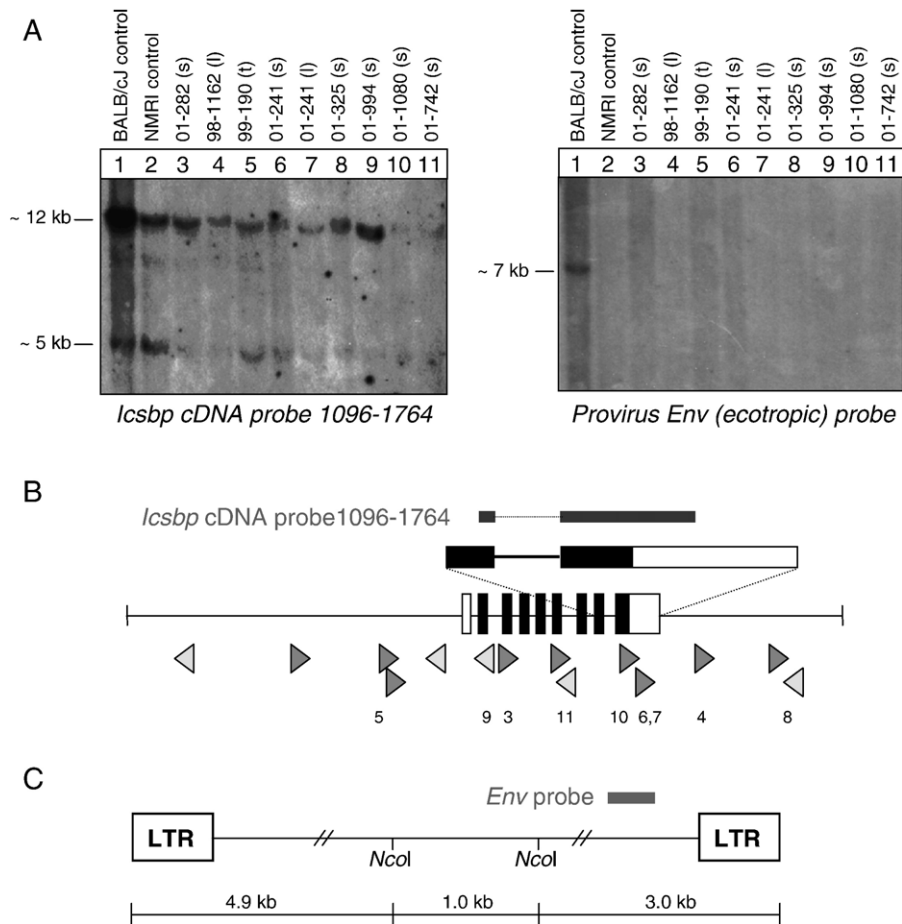


Fig. 2. Southern blot analyses of integrated proviruses. (A) Genomic DNAs from tumors harboring proviral integration in the *Icsbp* locus were isolated and digested with *NcoI* and hybridized with an *Icsbp* cDNA probe covering the integration sites located in exon 9 (tumor 01-241 and 01-1080) (left panel; probe location shown in panel B) or an ecotropic-specific MVLV probe (right panel; probe location shown in panel C). Lanes 1 and 2 are control DNAs from uninfected BALB/cJ and NMRI mice. BALB/cJ contains one copy of an endogenous ecotropic MLV (serving as positive control for the Env probe), while NMRI contains no endogenous ecotropic MLVs (serving as negative control for the Env probe). The l, t, and s (lymph node, thymus, and spleen, respectively) refer to the tumor tissues from which the DNA was isolated. (B) Location of the *Icsbp* cDNA probe 1096–1764. Numbers correspond to nucleotide positions in GenBank Accession Number M32489. The probe contains 23 bp of exon 8 and 643 bp of exon 9. Triangles below the map of the *Icsbp* locus illustrate (as in Fig. 1) positions and orientations of integrated proviruses with the numbers referring to lane numbers in panel A. (C) Schematic illustration of the proviral DNA with location of *Env* probe and *NcoI* restriction sites indicated.

of expression of a tumor-suppressor gene would provide an explanation of the apparent oncogenic role of the proviral integrations into *Icsbp*.

#### Chimeric *Icsbp*-retroviral transcripts in tumors

The two outstanding cases in the Northern-blot analyses represented the only cases where the provirus integrations took place inside the gene and within an exon. Tumors 01-1080 and 01-241 both harbored an integration in exon 9, the former in the *Icsbp* coding region and the latter in the 3' untranslated region (Fig. 1). Besides, both proviruses were integrated in the same transcriptional orientation as the *Icsbp* gene itself.

In the two exceptional cases, an altered expression pattern was revealed as compared to that of the other tumor samples; thus, in both instances, an additional, strongly expressed transcript could be observed. Regarding tumor 01-241, the size of the additional transcript was 2.1 kb (Fig. 5A); while in the case of tumor 01-1080, the size was estimated to be about

1.8 kb (Fig. 5B). The locations and orientations of the integrated proviruses, taken together with the sizes of the alternative transcripts observed by the Northern blotting hybridization, suggested that chimeric transcripts consisting of *Icsbp* as well as proviral sequences had been produced. In order to investigate this, RT-PCRs were performed on tumor RNA, with the usage of an *Icsbp*-specific upstream PCR primer together with a provirus-specific downstream PCR primer (primer locations depicted in Fig. 5). The results (shown in Fig. 5C) were amplified fragments of the expected sizes of 1452 bp and 1696 bp, respectively. Subsequent determination of the sequences confirmed the identity of the amplified fragments and established that they were composed 5' of truncated *Icsbp* sequences and 3' of proviral U3-R region, thus validating that the poly(A) signal in the 5'LTR of the provirus had been used in the production of the truncated *Icsbp* RNA.

In two additional tumor samples, a provirus was found inserted in a co-transcriptional orientation within the gene (01-742 and 01-282; Fig. 6), and hence a possibility for generating

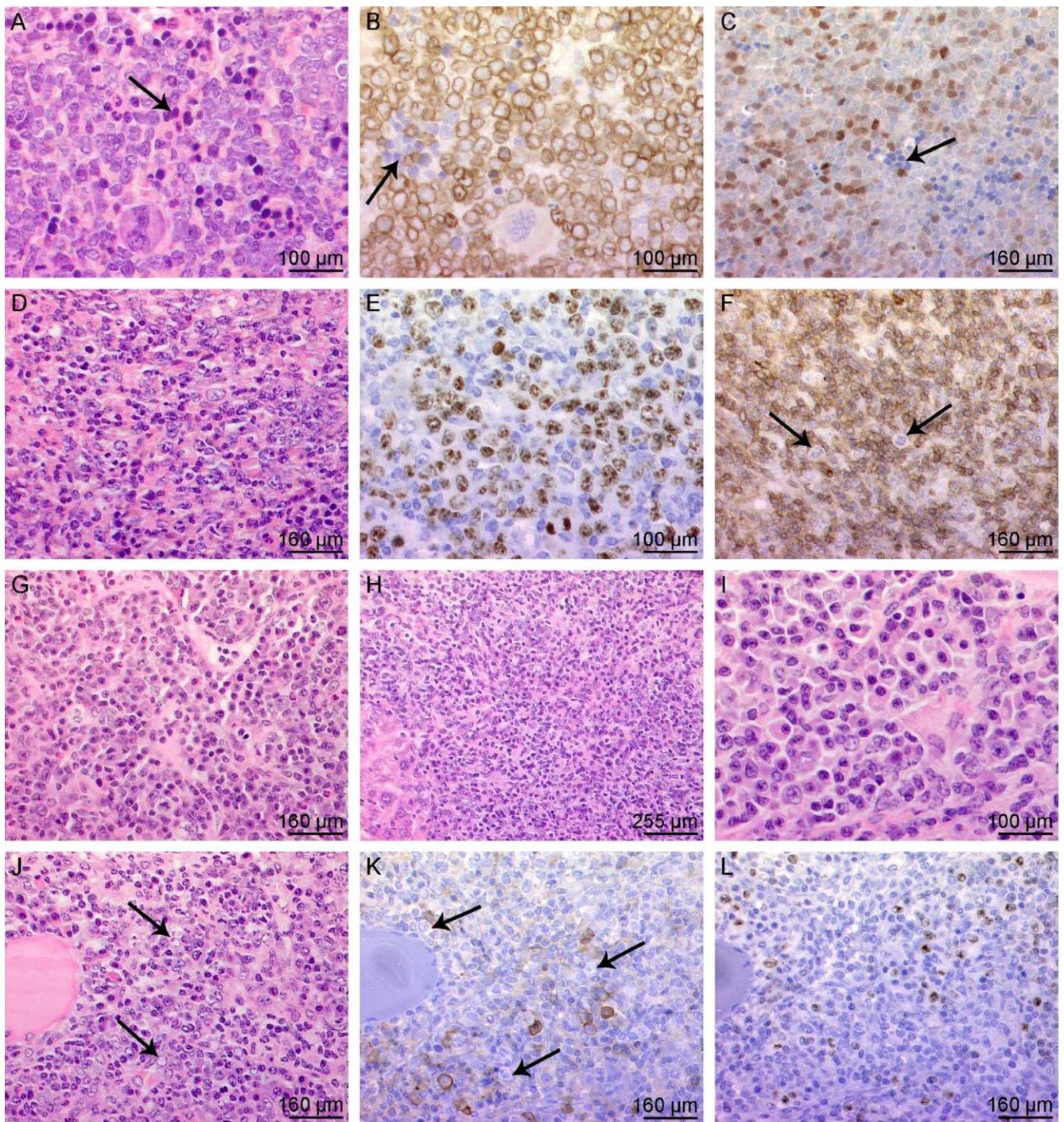


Fig. 3. Histological and immunohistological analyses of lymphoid neoplasias in retrovirus-infected NMRI mice. (A–C) A mouse infected with Akv1-99 (mEg<sub>re</sub> + mEa/s) developed a precursor T-cell lymphoblastic lymphoma. The tumor is composed of monotonous population of medium-sized cells with blastic chromatin. Arrows indicate areas of erythropoiesis. Neoplastic cells infiltrate the red and white pulp (A, H&E, spleen). The tumor cells are CD3-positive (B, thymus) and TdT-positive (C, thymus). (D–F) Representative pictures of a diffuse large B-cell lymphoma. The tumor cells are large with irregular-shaped nuclei, open chromatin, and abundant pale-stained cytoplasm (D, H&E, spleen). Ki-67 staining demonstrates a high proliferation rate in the neoplastic cells (E, spleen) that stained positive for B220 (data not shown). Many reactive CD3-positive T-cells are present (F, spleen). The large neoplastic cells are negative for CD3 (arrows). (G–I) Severe plasma cell proliferation is depicted. The infiltrate is present in the lymph nodes (G, H&E), liver (H, H&E), and spleen (I, H&E). In some cases, the plasma cells are intermingled with large cells (arrows) or centroblasts (J, H&E), which have irregular-shaped nuclei with open chromatin. These centroblastic-appearing cells are CD138-negative (K, arrows) and Ki-67-positive (L), suggesting progression of the disease.

chimeric transcripts was present also in these cases. However, in contrast to tumors 01-1080 and 01-241, the integration sites were located within an intron (intron 5 and intron 2,

respectively). Again, RT-PCRs were performed with *Icsbp*-specific upstream PCR primers together with a provirus-specific downstream PCR primer (Figs. 6A, B), resulting in amplified

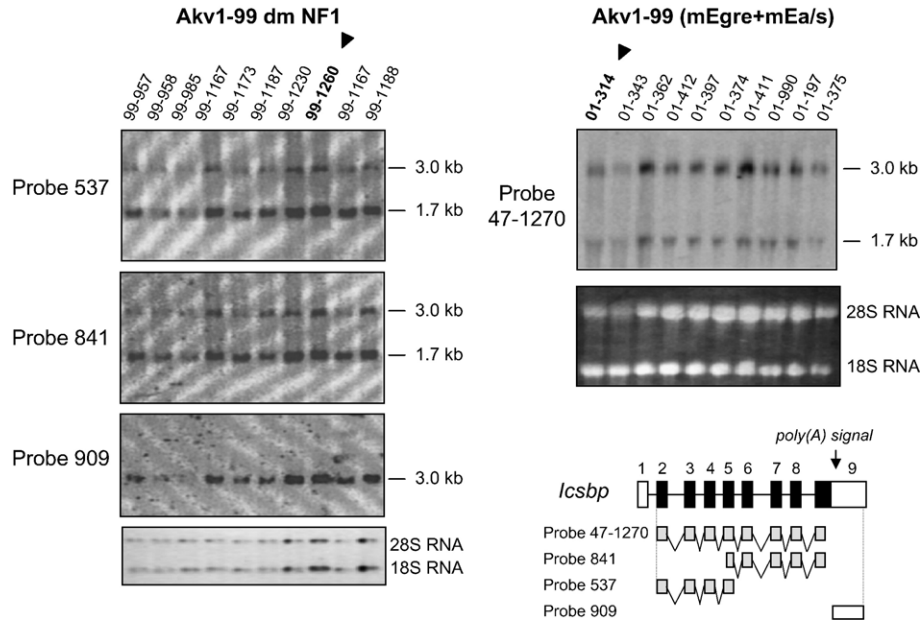


Fig. 4. Expression of long and short transcripts in tumors. Total RNA from 10 tumors induced by Akv1-99 dm NF1 and 10 tumors induced by Akv1-99 (mEgE + mEa/s) was analyzed by Northern blotting using four *Icsbp* cDNA probes, designated as 537, 841, 909, and 47-1270. Probes 537, 841, and 47-1270 detected two mRNAs of 3.0 kb and 1.7 kb, respectively, whereas probe 909 detected only the 3.0 kb transcript. The tumors with proviral insertions at *Icsbp* are marked in bold and with a triangle. Ethidium staining of 28S and 18S ribosomal RNA served as loading controls. The lower right panel depicts the structure of the cDNA probes in relation to the exon–intron organization of the *Icsbp* locus. A potential alternative poly(A) signal (ATTAAA) at position 1491–1496 of M32489 is indicated.

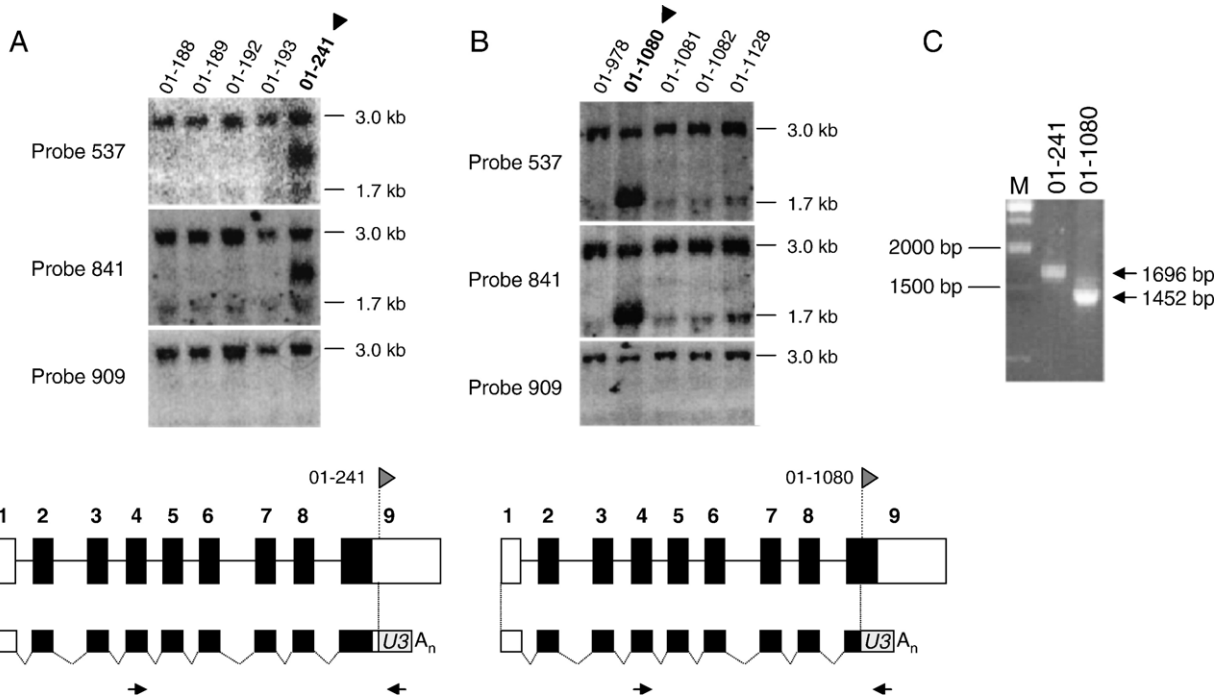


Fig. 5. Chimeric transcripts generated by proviral insertions into exon 9 of *Icsbp*. (A and B) Northern blot hybridization of RNAs from Akv wt (A) and Akv1-99 mEa/s (B) induced tumors with probes 537, 847, and 909. Probes 537 and 841 detected a 2.1 kb chimeric transcript in tumor 01-241 (A; top), and a 1.8 kb chimeric transcript in tumor 01-1080 (B; top). DNA of tumors 01-241 and 01-1080 contained a proviral integration in the 3'UTR sequence in exon 9 of *Icsbp* (A; bottom) and in the coding sequence in exon 9 of *Icsbp* (B; bottom), respectively. Black or white rectangles represent coding/noncoding exons of *Icsbp*, while grey rectangles represent provirus sequences in the recombinant transcripts. The flags denote insertion sites and the horizontal arrows the primers used for PCR analysis. (C) Total RNA extracted from tumors 01-1080 and 01-241 was reverse-transcribed using an oligo(dT)-primer. Products of subsequent RT-PCR reactions using the primer pairs shown in lower panels of A and B were analyzed by agarose gel electrophoresis.

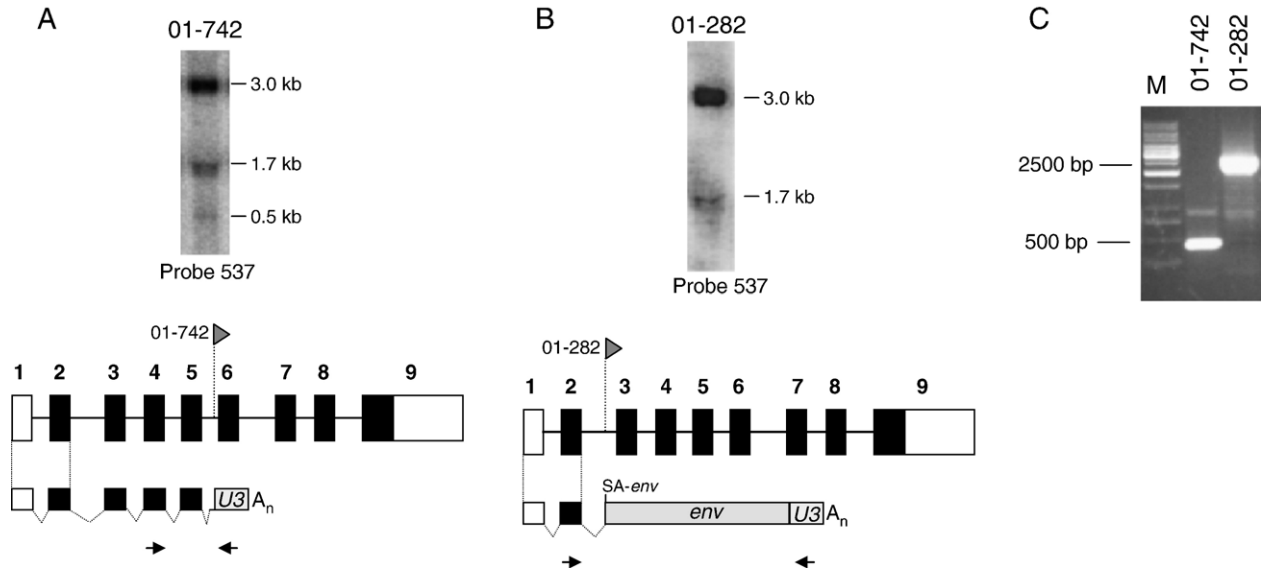


Fig. 6. Chimeric transcripts generated by proviral insertions into intron 2 and intron 5 of *Icsbp*. (A and B) Northern blot hybridization with probe 537 of RNA from tumors 01-742 (A; top) and 01-282 (B; top). Indicated are the 3.0 kb long transcript and the 1.7 kb short transcript. Recombinant transcripts detected in tumors 01-742 and 01-282 are illustrated in panels A and B (bottom). Black or white rectangles represent coding/noncoding exons of *Icsbp*, while grey rectangles represent provirus sequences in the recombinant transcripts. The flags denote insertion sites and the horizontal arrows the primers used for PCR analysis. (C) Total RNA from tumors 01-742 and 01-282 was reverse-transcribed using an oligo(dT)-primer, and the PCR products made using the primers depicted in panels A and B were analyzed by agarose gel electrophoresis. The bands were sequenced to reveal the recombinant RNA structures depicted in panels A and B.

fragments of 410 bp for tumor 01-742 and 2472 bp for tumor 01-282 (Fig. 6C). Sequence determination revealed that the chimeric transcript of tumor 01-742 contained *Icsbp* exons 1–5 which by usage of a cryptic splice splice-acceptor site in intron 5 were fused together with a small part (10 nucleotides) of intron 5 connected to the viral U3 region, and making use of the poly(A) signal in the 5'LTR of the provirus. Moreover, the Northern blotting hybridization (Fig. 6A) revealed an additional, yet weakly expressed transcript of about 0.5 kb, which probably corresponded to this transcript. In case of tumor sample 01-282, sequence determination of the PCR fragments revealed that the chimeric transcript was composed of *Icsbp* exons 1 and 2 spliced together with the 3' end of the integrated provirus. The splice-donor (SD) site of *Icsbp* exons 2 had been used together with the canonical splice-acceptor (SA) site in the provirus (the SA normally used to produce the spliced envelope transcript), thereby producing a composite transcript containing *Icsbp* exons 1–2 and an MLV envelope gene. However, the Northern blot hybridization (Fig. 6B) did not show specific bands corresponding to this transcript, either because it is co-migrating with the 3.0 kb band or because the copy number is too low for detection, considering that its only match with probe 537 is the sequence of exon 2.

Altogether, these analyses establish that in all cases where a provirus had integrated in a co-transcriptional orientation within the *Icsbp* gene, chimeric transcripts were produced; however, only when the integration took place within an exon was a substantial expression level observed. The significance of these findings is not clear in terms of qualitative or quantitative changes in ICSBP protein. However, they positively contribute to the notion that the *Icsbp* is indeed the gene, which has been

affected by the integrated proviruses, and which in a still unknown way is involved in B-cell lymphomagenesis.

#### *The ICSBP protein level in tumors is not generally affected by the proviral Icsbp insertions*

Since we found that the proviral *Icsbp* insertions in general did not significantly affect *Icsbp* RNA expression, we wanted to see if this was reflected in the ICSBP protein level in the tumor samples. Western blot analyses were performed on tumor samples of three series (comprising 3 tumors with and 12 tumors without insertion at the *Icsbp* locus) (Fig. 7), which resulted in the same overall picture as the Northern-blot analyses: in all tumor samples, a similar protein level was observed, which was not affected by the presence of an *Icsbp* provirus insertion. Only in the two cases where the insertions were found in *Icsbp* exon 9, was a slightly increased protein level detected, which may mirror the strongly expressed alternative transcripts observed in these tumors. The site of insertion in tumor 01-1080 predicts the formation of an ICSBP protein devoid of the last 5 amino acids, which may influence its detection by the antibody.

#### Discussion

Mouse models of retroviral insertional mutagenesis have become an essential cancer-gene discovery tool in the era of post genome-sequence completion. Making use of such a model of MLV-induced lymphomas in NMRI mice, in the present study we have identified 14 insertions within the *Icsbp* locus by a high-throughput sequencing approach—in which a total of approximately 3000 proviral integration sites were isolated.

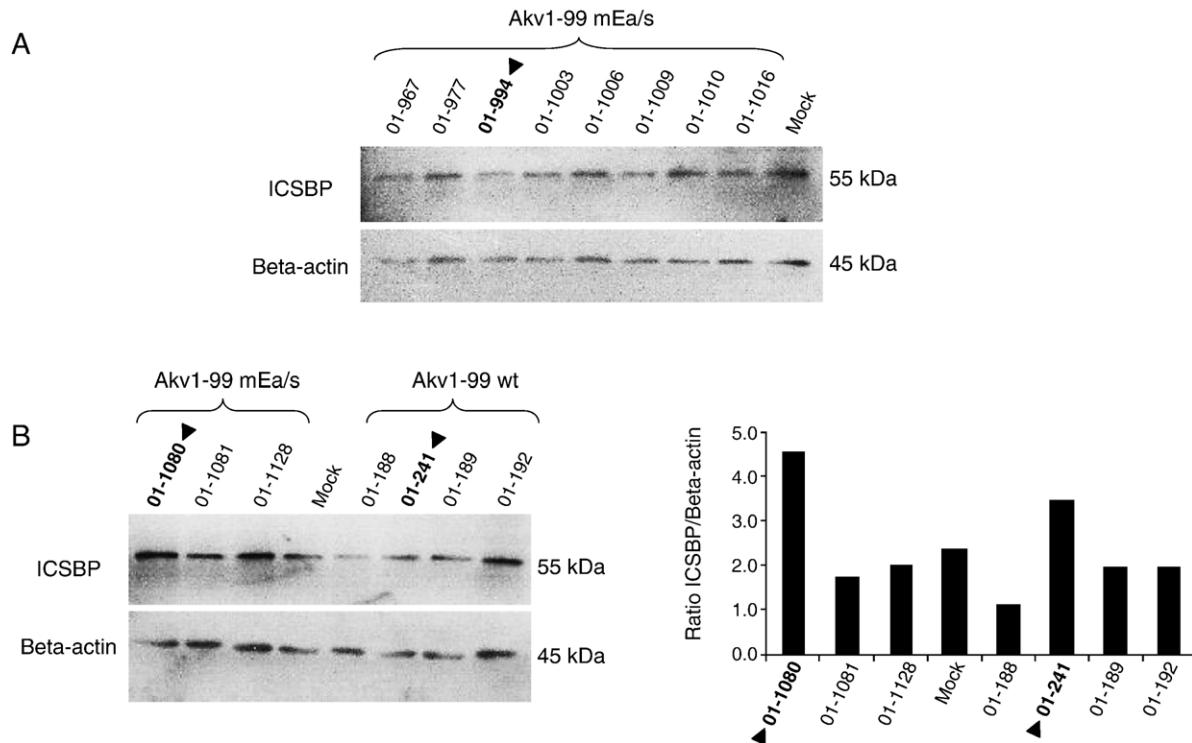


Fig. 7. Western blot analysis of ICSBP in tumors. Tumor tissues were homogenized and 10  $\mu$ g of protein was separated by SDS-polyacrylamide gel electrophoresis. After immunoblotting, protein levels were chemoluminescently detected. Beta-actin staining was used as a loading control. (A) Analysis of Akv1-99mEa/s-induced tumors; tumor 01-994 has a proviral insertion into intron 2 of *Icsbp*. (B) Analysis of Akv1-99 wt (lanes 1–4) and Akv1-99 mEa/s (lanes 5–8) induced tumors; tumors 01-241 and 01-1080 have proviral insertions in exon 9 outside and within the coding sequences, respectively (see Fig. 1). The right panel shows ICSBP/Beta-actin ratios determined by PhosphorImager analysis.

Searching the Retroviral Tagged Cancer Gene Database (RTCGD; <http://RTCGD.ncifcrf.gov>) Akagi et al., 2004) for previously identified proviral integrations in this locus revealed no such hits; thus *Icsbp* denotes a novel common integration site (CIS) as has been defined by Suzuki et al. (2002).

Remarkably, all but one of the integrations were found in tissues, which by Southern blot and histopathological analyses could be classified as being of B-cell origin despite the fact that about half of isolated proviral tags were derived from tumors of T-cell origin. This strongly implies a B-cell-restricted role of the *Icsbp* locus in the development of lymphoid malignancies. However, expression analyses of *Icsbp* in tumor tissues did not reveal any common pattern of changes in either RNA or protein levels when compared to equivalent tumor tissues with no *Icsbp* provirus insertions. Thus, it seems that the consequence of the integrations is not merely a matter of activation or suppression of ICSBP expression, which in turn would have led to an oncogenic development. On the other hand, the expression analyses were performed on end-stage tumor tissues, so it cannot be ruled out that a disturbance of expression might have taken place earlier on in the progression of the tumors. Such an early disturbance might somehow have put a selection pressure to the cells that eventually might have expanded and transformed into malignant clones. Nevertheless, the stable *Icsbp* expression that we observed in MLV-induced lymphomas is in sharp contrast to what has been reported for the myeloid cancers in which *Icsbp* seems to hold a tumor suppressor

activity as demonstrated by ICSBP down regulation in cancer tissues (Hao and Ren, 2000; Schmidt et al., 2004). Hence, this supports a view that the cancer-related function of ICSBP depends very much on the cell-type context.

Alternatively, one may argue that the reason why no expression alterations can be detected in the MLV-induced lymphomas could be that it is not at all the *Icsbp* gene itself which is affected by the integrated proviruses. It is well-known that integrated proviruses may influence genes that are located several hundreds kilobase away from the insertion sites (Lazo et al., 1990). Accordingly, the actual target gene may be one of the neighboring genes (depicted in Fig. 1). However, this seems not to be a plausible explanation for several reasons. First and foremost, the extremely distinct pattern of clustering around and within the *Icsbp* gene quite convincingly points to *Icsbp* as the target gene. Second, the chimeric transcripts that were produced and heavily expressed when the integrations were located in *Icsbp* exon sequences further add support to this gene being the central one, and at last, our expression analyses of the two most closely situated genes, *Cox4i1* and *Cox4nb* (data not shown), did not reveal changes in expression pattern. Likewise, a search for mouse microRNAs within the 100 kb window at *Icsbp* at <http://www.sanger.ac.uk/Software/Rfam/mirna/> did not reveal any candidates. Hence, the most obvious deduction is that *Icsbp* is indeed the target gene.

Currently, more than 2200 RISs and almost 400 CISs are contained in the RTCG database. Some of the CISs appear to be

restricted to specific disease phenotypes, while others seem to play a role in a wider range of cell types. Moreover, the frequency with which the individual CISs are targeted depends very much on the model system, i.e. mouse strain and type of retrovirus. For example, both Moloney and SL3-3 MLVs induce T-cell lymphomas, but their mutual relative strengths vary with the host-genetic background, and so does the pattern of preferred target genes (Blyth et al., 2001; Kim et al., 2003; Mikkers et al., 2002a, 2002b; Nielsen et al., 2005). This fact may contribute to a clarification of the quite unexpected finding that *Icsbp* could not be found in the RTCGD, not even as an RIS, although about half of the CISs in the database can be correlated with B-cell malignancies. The majority of the B-cell-related CISs do in fact originate from Akv or Akv-related proviral integrations, but in contrast to the present study, tumor induction has in all cases been caused by expression of an endogenous MLV, yet in various mouse genetic backgrounds such as AKR, AKXD, NFS.V+, CWD, SJL/J, and SL/Kh mice (Gilbert et al., 1993; Hartley et al., 2000; Mucenski et al., 1986; Yamada et al., 1994). Thus, a straightforward explanation of the lack of *Icsbp* hits in RTCGD would be that the genetic composition in the NMRI strain somehow makes these mice more prone to tumor induction by Akv proviral insertions in the *Icsbp* locus.

Since all known B-cell-related CISs are correlated with endogenous MLV tumor induction, an alternative explanation could be suggested. An exogenous MLV might trigger an early ICSBP-affected modulation of an immune response, which at the same time may play a role in the initiation and/or progression of B-cell tumor development. Infection within the first 2 to 3 days after birth is critical for lymphomagenesis by exogenous MLVs. Although the establishment of some level of immunological tolerance by such early infection is important to allow progression of viral replication, the mechanisms are poorly understood, and it is conceivable that the virus may elicit innate and adaptive immune response signaling (Sarzotti et al., 1996). MLVs and other retroviruses have been found to interact with Toll-like receptors, which are important for an early innate host response to viral infections (Rassa et al., 2002). Likewise, the transmembrane protein of MLV harbors an immunosuppressive peptide motif with an influence on immune signaling, although the exact signaling pathways are poorly defined (Haraguchi et al., 1995). An early innate immune response to exogenous MLV might skew a delicate balance of cytokines and push the cells to an increased proliferation stage. The constitutive expression of *Icsbp* modulates NF- $\kappa$ B stimulation through toll-like receptor (TLR) signaling, which could lead to tumor survival and inhibition of apoptosis (Bernal et al., 2001; Cahir-McFarland et al., 2000; Darnell, 2002). ICSBP might also be involved in these processes by regulating IL-12 production. In these settings, cells with deregulated expression of *Icsbp* as a result of proviral insertions at the locus may be favored.

We have previously observed plasma cell proliferation and plasmacytoma induction following infection of newborn mice of the inbred NMRI strain with the Akv1-99 virus and proposed that this disease model may have an antigen-stimulatory

component (Sorensen et al., 2005). The inbred NMRI strain appears particularly prone to lymphoma induction by exogenous Akv and related viruses (Sorensen et al., 2005), possibly reflecting an influence of the genetic composition of this mouse strain on the regulation of innate or adaptive immune responses. An expanded cell population would gain an increased probability for additional insertional mutagenesis events, which could serve to further stimulate growth in an autocrine or paracrine manner or represent a genuine transformation event. Such processes could lead to the outgrowth of polyclonal or oligo-/monoclonal tumors of malignant or chronically stimulated cells.

The model presented here with the frequent targeting of the *Icsbp* locus preferentially in B-cell lymphomas induced by an exogenous MLV, and the steady RNA/protein expression in tumor tissues may add an interesting experimental approach for future investigations of links between an innate or adaptive immune response and the development of B-cell lymphomas.

## Materials and methods

### *Origin of lymphomas and MLV variants*

Mouse lymphomas induced by wt and mutants of Akv and SL3-3 MLVs (from a total of 1203 mice) were available from our earlier and unpublished work (Ethelberg et al., 1997, 1999; Hallberg et al., 1991; Lovmand et al., 1998, 1990; Lund et al., 1999; Sorensen et al., 1996, 2000, 2005). In short, newborn inbred NMRI mice were injected with approximately  $10^5$  infectious virus particles, and the mice were sacrificed when they showed signs of illness (Schmidt et al., 1988). Spleen, thymus, and lymph nodes were dissected and measured, and samples were immediately frozen at  $-80$  °C. Tumor development was diagnosed on the basis of grossly enlarged lymphatic organs (the defined sizes have been described previously; Schmidt et al., 1984). The tumors found positive for insertions at the *Icsbp* locus were induced by the following viruses: Akv wild type (Akv wt), an Akv primer binding site (PBS) mutant, an Akv gag splice mutant, five different Akv U3 enhancer mutants (Akv1-99 NF1 dm, Akv1-99 wt, Akv1-99 mRunx + mEgre, Akv1-99 mEgre + mEa/s, and Akv1-99 mEa/s), and finally, one attenuated SL3-3 variant (SL3-3 Runx dm) (description of virus structures have been described previously/will be described elsewhere; Ethelberg et al., 1997, 1999; Hallberg et al., 1991; Lovmand et al., 1998, 1990; Lund et al., 1999; Olsen et al., 1990; Sorensen et al., 2005).

### *Provirus tagging and statistical analyses*

1203 mouse tumors were screened for proviral insertion sites at Sagres Discovery, Inc. (California, USA) using high-throughput provirus tagging procedures (Rasmussen et al., 2005). Assuming a random distribution of 3000 retroviral integrations into the mouse genome ( $3 \times 10^9$  bp), the expected frequency of tagging a site within the *Icsbp* locus

( $1 \times 10^5$  bp) would be 0.1. According to the Poisson distribution

$$P(X = \chi) = \frac{\mu^\chi e^{-\mu}}{\chi!}$$

where  $\mu$  is the frequency of random-tagged sites in the mouse genome, and  $\chi$  is the frequency of observed tagged sites in the 100 kb *Icsbp* locus.

#### Histopathological examination

Hematoxylin and eosin (H&E) sections from formalin- or paraformaldehyde-fixed and paraffin-embedded tissue (lymph nodes, thymus spleen, and liver) were revised for all tumors found to be positive for insertion at the *Icsbp* locus. In addition, immunohistochemical stains were carried out for these 14 cases. Tumors were classified according to the Bethesda proposals for classification of lymphoid neoplasms in mice (Morse et al., 2002). Immunohistochemistry was performed on an automated immunostainer (Ventana Medical System, Inc.; AZ, USA), according to the protocol provided by the company with slight modifications. After deparaffinization and rehydration, the slides were placed in a microwave pressure cooker in 0.01 M citrate buffer (pH 6.0), containing 0.1% Tween 20 and heated in a microwave oven at maximum power for 30 min. After cooling in Tris-buffered saline, the sections were incubated with 3% goat or rabbit serum for 20 min. The antibody panel used included polyclonal anti-CD3, monoclonal anti-CD79acy, and monoclonal anti-TdT (Dako, Germany); polyclonal anti-Bcl6 (Santa Cruz, CA, USA); monoclonal rat anti-CD138 and anti-B220/CD45R (BD Bioscience, NJ, USA); and monoclonal rabbit anti-ki67 (DCS, Germany). Appropriate positive controls were used to confirm the adequacy of the staining.

#### Southern blotting analyses

Genomic DNA was extracted from frozen tissues, digested with *Hind*III or *Eco*RI, electrophoretically separated on a 0.8% agarose gel, blotted onto a nylon membrane (Amersham Biosciences), and hybridized with the following  $^{32}$ P random priming labeled probes: T-cell receptor (TCR)- $\beta$  chain joining region 1 (TCR-J1) and region 2 (TCR-J2) probes, immunoglobulin kappa light-chain (Ig $\kappa$ ) probe, immunoglobulin heavy-chain (IgH) probe, and an ecotropic-specific envelope probe (all probes and hybridization procedures have been described earlier by Lovmand et al., 1998).

#### Northern blotting analyses

Total RNA was extracted from frozen tumor tissues using TRIzol reagent according to the manufacturer's instructions (Invitrogen Life Technologies). For Northern blotting, 20  $\mu$ g of total RNA was electrophoretically separated on a denaturing 1% agarose gel (1 $\times$  MOPS, 6.7% formaldehyde) and transferred to a positively charged nylon membrane (Amersham Biosciences) by capillary action, fixed, prehybridized, and hybridized with

$^{32}$ P random priming labeled probes corresponding to *Icsbp* cDNA fragments, named probe 537 (covers nts 47-558 of GenBank accession number M32489), probe 841 (covers nts 453-1293 of M32489), probe 909 (covers nts 1462-2370 of M32489), and probe 47-1270 (covers nts 47-1270 of M32489). Hybridization and washing procedures have previously been described (Sorensen et al., 2000). The integrity and concentration of the RNA were confirmed/estimated by visual inspection of ethidium bromide-stained 18S and 28S rRNAs.

#### RT-PCR and sequencing

For RT-PCR, 600 ng total RNA was used to make first-strand cDNA (Amersham Biosciences) with oligo-dT primer, followed by PCR amplification using a MLV ecotropic-specific downstream primer and *Icsbp*-specific upstream primers. The downstream ecotropic MLV primer was: 2620; 5'-GAATTC-GATATCGATCCCCGGTCATCTGGG-3' (Lovmand et al., 1998; Sorensen et al., 1993); *Icsbp*-specific primers were: 47; 5'-GCTGCGGCAGTGGCTGATCGAACAGATCG-3', and 453; 5'-GAGCTGATCAAGGAACCTTCTGTG-3'. PCR products were purified with GFX, and sequences were determined by the use of ABI 7300 Biosystems.

#### Western blotting analyses

Equal amounts of proteins (10  $\mu$ g) were separated by (SDS-PAGE), and electro-blotted onto polyvinylidene fluoride (PVDF) membranes (Boehringer Mannheim). The membrane was blocked in TBS (20 mM Tris, 137 mM NaCl, pH 7.6) (TBS) containing 3% BSA. Membranes were then incubated for 1 h with 1:6000 dilution of affinity-purified goat polyclonal anti-mouse ICSBP antibody directed against the C-terminal 17 amino acid-peptide of the protein (Sc-6058) (Santa Cruz Biotechnology, Inc.) in TBS containing 0.05% Tween-20 (TBST) and 3% BSA. After five washes with wash buffer (TBS, 0.01% Tween-20, 0.1% BSA), membranes were incubated with 1:2000 dilutions of horseradish peroxidase (HRP)-linked secondary antibody of rabbit anti-goat immunoglobulins/HRP (DAKO A/S, Denmark) in PBST containing 3% BSA. Then the membranes were washed in wash buffer, and Western detection of ICSBP was conducted using the ECL Plus Western Blotting Detection System (Amersham Biosciences). Blots were exposed to Konica Medical film (Konica Minolta Medical and Graphic Inc.). After stripping, membranes were reincubated with 1:6000 dilutions of goat polyclonal anti-human  $\beta$ -actin antibody (I-19) (Santa Cruz Biotechnology, Inc.) for internal control of total protein loading.

#### Acknowledgments

The assistance of Claudia Kloß, Nadine Kink, Jacqueline Müller, and Elenore Samson with the immunohistochemical and histological preparations is gratefully acknowledged.

This work was supported by grants from the Danish Cancer Society, the Novo Nordic Foundation, the Karen Elise Jensen Foundation, and the Danish Medical Research Council.

## References

- Akagi, K., Suzuki, T., Stephens, R.M., Jenkins, N.A., Copeland, N.G., 2004. RTCGD: retroviral tagged cancer gene database. *Nucleic Acids Res.* 32, D523–D527 (Database issue).
- Bernal, A., Pastore, R.D., Asgary, Z., Keller, S.A., Cesarman, E., Liou, H.C., Schattner, E.J., 2001. Survival of leukemic B cells promoted by engagement of the antigen receptor. *Blood* 98 (10), 3050–3057.
- Blyth, K., Terry, A., Mackay, N., Vaillant, F., Bell, M., Cameron, E.R., Neil, J.C., Stewart, M., 2001. Runx2: a novel oncogenic effector revealed by *in vivo* complementation and retroviral tagging. *Oncogene* 20 (3), 295–302.
- Bovolenta, C., Driggers, P.H., Marks, M.S., Medin, J.A., Politis, A.D., Vogel, S.N., Levy, D.E., Sakaguchi, K., Appella, E., Coligan, J.E., et al., 1994. Molecular interactions between interferon consensus sequence binding protein and members of the interferon regulatory factor family. *Proc. Natl. Acad. Sci. U.S.A.* 91 (11), 5046–5050.
- Cahir-McFarland, E.D., Davidson, D.M., Schauer, S.L., Duong, J., Kieff, E., 2000. NF-kappa B inhibition causes spontaneous apoptosis in Epstein–Barr virus-transformed lymphoblastoid cells. *Proc. Natl. Acad. Sci. U.S.A.* 97 (11), 6055–6060.
- Contursi, C., Wang, I.M., Gabriele, L., Gadina, M., O’Shea, J., Morse III, H.C., Ozato, K., 2000. IFN consensus sequence binding protein potentiates STAT1-dependent activation of IFN-gamma-responsive promoters in macrophages. *Proc. Natl. Acad. Sci. U.S.A.* 97 (1), 91–96.
- Darnell III, J.E., 2002. Transcription factors as targets for cancer therapy. *Nat. Rev., Cancer* 2 (10), 740–749.
- Darnell Jr., J.E., Kerr, I.M., Stark, G.R., 1994. Jak-STAT pathways and transcriptional activation in response to IFNs and other extracellular signaling proteins. *Science* 264 (5164), 1415–1421.
- Driggers, P.H., Ennist, D.L., Gleason, S.L., Mak, W.H., Marks, M.S., Levi, B.Z., Flanagan, J.R., Appella, E., Ozato, K., 1990. An interferon gamma-regulated protein that binds the interferon-inducible enhancer element of major histocompatibility complex class I genes. *Proc. Natl. Acad. Sci. U.S.A.* 87 (10), 3743–3747.
- Driggers, P.H., Elenbaas, B.A., An, J.B., Lee, I.J., Ozato, K., 1992. Two upstream elements activate transcription of a major histocompatibility complex class I gene *in vitro*. *Nucleic Acids Res.* 20 (10), 2533–2540.
- Eisenbeis, C.F., Singh, H., Storb, U., 1995. Pip, a novel IRF family member, is a lymphoid-specific, PU.1-dependent transcriptional activator. *Genes Dev.* 9 (11), 1377–1387.
- Eklund, E.A., Kakar, R., 1999. Recruitment of CREB-binding protein by PU.1, IFN-regulatory factor-1, and the IFN consensus sequence-binding protein is necessary for IFN-gamma-induced p67phox and gp91phox expression. *J. Immunol.* 163 (11), 6095–6105.
- Ethelberg, S., Hallberg, B., Lovmand, J., Schmidt, J., Luz, A., Grundstrom, T., Pedersen, F.S., 1997. Second-site proviral enhancer alterations in lymphomas induced by enhancer mutants of SL3-3 murine leukemia virus: negative effect of nuclear factor 1 binding site. *J. Virol.* 71 (2), 1196–1206.
- Ethelberg, S., Tzschaschel, B.D., Luz, A., Diaz-Cano, S.J., Pedersen, F.S., Schmidt, J., 1999. Increased induction of osteopetrosis, but unaltered lymphomagenicity, by murine leukemia virus SL3-3 after mutation of a nuclear factor 1 site in the enhancer. *J. Virol.* 73 (12), 10406–10415.
- Gilbert, D.J., Neumann, P.E., Taylor, B.A., Jenkins, N.A., Copeland, N.G., 1993. Susceptibility of AKXD recombinant inbred mouse strains to lymphomas. *J. Virol.* 67 (4), 2083–2090.
- Hallberg, B., Schmidt, J., Luz, A., Pedersen, F.S., Grundstrom, T., 1991. SL3-3 enhancer factor 1 transcriptional activators are required for tumor formation by SL3-3 murine leukemia virus. *J. Virol.* 65 (8), 4177–4178.
- Hansen, G.M., Skapura, D., Justice, M.J., 2000. Genetic profile of insertion mutations in mouse leukemias and lymphomas. *Genome Res.* 10 (2), 237–243.
- Hao, S.X., Ren, R., 2000. Expression of interferon consensus sequence binding protein (ICSBP) is downregulated in Bcr-Abl-induced murine chronic myelogenous leukemia-like disease, and forced coexpression of ICSBP inhibits Bcr-Abl-induced myeloproliferative disorder. *Mol. Cell. Biol.* 20 (4), 1149–1161.
- Harada, H., Fujita, T., Miyamoto, M., Kimura, Y., Maruyama, M., Furia, A., Miyata, T., Taniguchi, T., 1989. Structurally similar but functionally distinct factors, IRF-1 and IRF-2, bind to the same regulatory elements of IFN and IFN-inducible genes. *Cell* 58 (4), 729–739.
- Haraguchi, S., Good, R.A., James-Yarish, M., Cianciolo, G.J., Day, N.K., 1995. Differential modulation of Th1- and Th2-related cytokine mRNA expression by a synthetic peptide homologous to a conserved domain within retroviral envelope protein. *Proc. Natl. Acad. Sci. U.S.A.* 92 (8), 3611–3615.
- Hartley, J.W., Chattopadhyay, S.K., Lander, M.R., Taddesse-Heath, L., Naghashfar, Z., Morse III, H.C., Fredrickson, T.N., 2000. Accelerated appearance of multiple B cell lymphoma types in NFS/N mice congenic for ecotropic murine leukemia viruses. *Lab. Invest.* 80 (2), 159–169.
- Holtschke, T., Lohler, J., Kanno, Y., Fehr, T., Giese, N., Rosenbauer, F., Lou, J., Knobloch, K.P., Gabriele, L., Waring, J.F., Bachmann, M.F., Zinkernagel, R.M., Morse III, H.C., Ozato, K., Horak, I., 1996. Immunodeficiency and chronic myelogenous leukemia-like syndrome in mice with a targeted mutation of the ICSBP gene. *Cell* 87 (2), 307–317.
- Jonkers, J., Berns, A., 1996. Retroviral insertional mutagenesis as a strategy to identify cancer genes. *Biochim. Biophys. Acta* 1287 (1), 29–57.
- Kakar, R., Kautz, B., Eklund, E.A., 2005. JAK2 is necessary and sufficient for interferon-gamma-induced transcription of the gene encoding gp91PHOX. *J. Leukocyte Biol.* 77 (1), 120–127.
- Kessler, D.S., Levy, D.E., Darnell Jr., J.E., 1988. Two interferon-induced nuclear factors bind a single promoter element in interferon-stimulated genes. *Proc. Natl. Acad. Sci. U.S.A.* 85 (22), 8521–8525.
- Kim, R., Trubetskoy, A., Suzuki, T., Jenkins, N.A., Copeland, N.G., Lenz, J., 2003. Genome-based identification of cancer genes by proviral tagging in mouse retrovirus-induced T-cell lymphomas. *J. Virol.* 77 (3), 2056–2062.
- Klemsz, M.J., McKercher, S.R., Celada, A., Van Beveren, C., Maki, R.A., 1990. The macrophage and B cell-specific transcription factor PU.1 is related to the ets oncogene. *Cell* 61 (1), 113–124.
- Lazo, P.A., Lee, J.S., Tschlis, P.N., 1990. Long-distance activation of the Myc protooncogene by provirus insertion in Mlvi-1 or Mlvi-4 in rat T-cell lymphomas. *Proc. Natl. Acad. Sci. U.S.A.* 87 (1), 170–173.
- Lee, C.H., Melchers, M., Wang, H., Torrey, T.A., Slota, R., Qi, C.F., Kim, J.Y., Lugar, P., Kong, H.J., Farrington, L., van der Zouwen, B., Zhou, J.X., Lougaris, V., Lipsky, P.E., Grammer, A.C., Morse III, H.C., 2006. Regulation of the germinal center gene program by interferon (IFN) regulatory factor 8/IFN consensus sequence-binding protein. *J. Exp. Med.* 203 (1), 63–72.
- Levi, B.Z., Hashmueli, S., Gleit-Kielmanowicz, M., Azriel, A., Meraro, D., 2002. ICSBP/IRF-8 transactivation: a tale of protein–protein interaction. *J. Interferon Cytokine Res.* 22 (1), 153–160.
- Lovmand, S., Kjeldgaard, N.O., Jorgensen, P., Pedersen, F.S., 1990. Enhancer functions in U3 of Akv virus: a role for cooperativity of a tandem repeat unit and its flanking DNA sequences. *J. Virol.* 64 (7), 3185–3191.
- Lovmand, J., Sorensen, A.B., Schmidt, J., Ostergaard, M., Luz, A., Pedersen, F.S., 1998. B-Cell lymphoma induction by akv murine leukemia viruses harboring one or both copies of the tandem repeat in the U3 enhancer. *J. Virol.* 72 (7), 5745–5756.
- Lu, R., Medina, K.L., Lancki, D.W., Singh, H., 2003. IRF-4,8 orchestrate the pre-B-to-B transition in lymphocyte development. *Genes Dev.* 17 (14), 1703–1708.
- Lund, A.H., Schmidt, J., Luz, A., Sorensen, A.B., Duch, M., Pedersen, F.S., 1999. Replication and pathogenicity of primer binding site mutants of SL3-3 murine leukemia viruses. *J. Virol.* 73 (7), 6117–6122.
- Marecki, S., Riendeau, C.J., Liang, M.D., Fenton, M.J., 2001. PU.1 and multiple IFN regulatory factor proteins synergize to mediate transcriptional activation of the human IL-1 beta gene. *J. Immunol.* 166 (11), 6829–6838.
- Martin-Hernandez, J., Sorensen, A.B., Pedersen, F.S., 2001. Murine leukemia virus proviral insertions between the N-ras and unr genes in B-cell lymphoma DNA affect the expression of N-ras only. *J. Virol.* 75 (23), 11907–11912.
- Meraro, D., Hashmueli, S., Koren, B., Azriel, A., Oumard, A., Kirchhoff, S., Hauser, H., Nagulapalli, S., Atchison, M.L., Levi, B.Z., 1999. Protein–protein and DNA–protein interactions affect the activity of lymphoid-specific IFN regulatory factors. *J. Immunol.* 163 (12), 6468–6478.
- Mikkers, H., Allen, J., Berns, A., 2002a. Proviral activation of the tumor

- suppressor E2a contributes to T cell lymphomagenesis in EmuMyc transgenic mice. *Oncogene* 21 (43), 6559–6566.
- Mikkers, H., Allen, J., Knipscheer, P., Romeijn, L., Hart, A., Vink, E., Berns, A., 2002b. High-throughput retroviral tagging to identify components of specific signaling pathways in cancer. *Nat. Genet.* 32 (1), 153–159.
- Morse III, H.C., Anver, M.R., Fredrickson, T.N., Haines, D.C., Harris, A.W., Harris, N.L., Jaffe, E.S., Kogan, S.C., MacLennan, I.C., Pattengale, P.K., Ward, J.M., 2002. Bethesda proposals for classification of lymphoid neoplasms in mice. *Blood* 100 (1), 246–258.
- Mucenski, M.L., Taylor, B.A., Jenkins, N.A., Copeland, N.G., 1986. AKXD recombinant inbred strains: models for studying the molecular genetic basis of murine lymphomas. *Mol. Cell. Biol.* 6 (12), 4236–4243.
- Nagamura-Inoue, T., Tamura, T., Ozato, K., 2001. Transcription factors that regulate growth and differentiation of myeloid cells. *Int. Rev. Immunol.* 20 (1), 83–105.
- Nelson, N., Marks, M.S., Driggers, P.H., Ozato, K., 1993. Interferon consensus sequence-binding protein, a member of the interferon regulatory factor family, suppresses interferon-induced gene transcription. *Mol. Cell. Biol.* 13 (1), 588–599.
- Nielsen, A.A., Sorensen, A.B., Schmidt, J., Pedersen, F.S., 2005. Analysis of wild-type and mutant SL3-3 murine leukemia virus insertions in the *c-myc* promoter during lymphomagenesis reveals target site hot spots, virus-dependent patterns, and frequent error-prone gap repair. *J. Virol.* 79 (1), 67–78.
- Olsen, H.S., Lovmand, S., Lovmand, J., Jorgensen, P., Kjeldgaard, N.O., Pedersen, F.S., 1990. Involvement of nuclear factor I-binding sites in control of Akv virus gene expression. *J. Virol.* 64 (9), 4152–4161.
- Rao, S., Garrett-Sinha, L.A., Yoon, J., Simon, M.C., 1999. The Ets factors PU.1 and Spi-B regulate the transcription *in vivo* of P2Y10, a lymphoid restricted heptahelical receptor. *J. Biol. Chem.* 274 (48), 34245–34252.
- Rasmussen, M.H., Sorensen, A.B., Morris, D.W., Dutra, J.C., Engelhard, E.K., Wang, C.L., Schmidt, J., Pedersen, F.S., 2005. Tumor model-specific proviral insertional mutagenesis of the *Fos/Jdp2/Batf* locus. *Virology* 337 (2), 353–364.
- Rassa, J.C., Meyers, J.L., Zhang, Y., Kudravalli, R., Ross, S.R., 2002. Murine retroviruses activate B cells via interaction with toll-like receptor 4. *Proc. Natl. Acad. Sci. U.S.A.* 99 (4), 2281–2286.
- Rehli, M., Poltorak, A., Schwarzfischer, L., Krause, S.W., Andreesen, R., Beutler, B., 2000. PU.1 and interferon consensus sequence-binding protein regulate the myeloid expression of the human Toll-like receptor 4 gene. *J. Biol. Chem.* 275 (13), 9773–9781.
- Sarzotti, M., Robbins, D.S., Hoffman, P.M., 1996. Induction of protective CTL responses in newborn mice by a murine retrovirus. *Science* 271 (5256), 1726–1728.
- Schiavoni, G., Mattei, F., Sestili, P., Borghi, P., Venditti, M., Morse, III, H.C., Belardelli, F., Gabriele, L., 2002. ICSBP is essential for the development of mouse type I interferon-producing cells and for the generation and activation of CD8alpha(+) dendritic cells. *J. Exp. Med.* 196 (11), 1415–1425.
- Schmidt, J., Erfle, V., Pedersen, F.S., Rohmer, H., Schettler, H., Marquart, K.H., Luz, A., 1984. Oncogenic retrovirus from spontaneous murine osteomas: I. Isolation and biological characterization. *J. Gen. Virol.* 65 (Pt. 12), 2237–2248.
- Schmidt, J., Luz, A., Erfle, V., 1988. Endogenous murine leukemia viruses: frequency of radiation-activation and novel pathogenic effects of viral isolates. *Leuk. Res.* 12 (5), 393–403.
- Schmidt, M., Nagel, S., Proba, J., Thiede, C., Ritter, M., Waring, J.F., Rosenbauer, F., Huhn, D., Wittig, B., Horak, I., Neubauer, A., 1998. Lack of interferon consensus sequence binding protein (ICSBP) transcripts in human myeloid leukemias. *Blood* 91 (1), 22–29.
- Schmidt, M., Bies, J., Tamura, T., Ozato, K., Wolff, L., 2004. The interferon regulatory factor ICSBP/IRF-8 in combination with PU.1 up-regulates expression of tumor suppressor p15(Ink4b) in murine myeloid cells. *Blood* 103 (11), 4142–4149.
- Sharf, R., Azriel, A., Lejbkowitz, F., Winograd, S.S., Ehrlich, R., Levi, B.Z., 1995. Functional domain analysis of interferon consensus sequence binding protein (ICSBP) and its association with interferon regulatory factors. *J. Biol. Chem.* 270 (22), 13063–13069.
- Sorensen, A.B., Duch, M., Jorgensen, P., Pedersen, F.S., 1993. Amplification and sequence analysis of DNA flanking integrated proviruses by a simple two-step polymerase chain reaction method. *J. Virol.* 67 (12), 7118–7124.
- Sorensen, A.B., Duch, M., Amtoft, H.W., Jorgensen, P., Pedersen, F.S., 1996. Sequence tags of provirus integration sites in DNAs of tumors induced by the murine retrovirus SL3-3. *J. Virol.* 70 (6), 4063–4070.
- Sorensen, A.B., Lund, A.H., Ethelberg, S., Copeland, N.G., Jenkins, N.A., Pedersen, F.S., 2000. Sint1, a common integration site in SL3-3-induced T-cell lymphomas, harbors a putative proto-oncogene with homology to the septin gene family. *J. Virol.* 74 (5), 2161–2168.
- Sorensen, K.D., Sorensen, A.B., Quintanilla-Martinez, L., Kunder, S., Schmidt, J., Pedersen, F.S., 2005. Distinct roles of enhancer nuclear factor 1 (NF1) sites in plasmacytoma and osteopetrosis induction by Akv1-99 murine leukemia virus. *Virology* 334 (2), 234–244.
- Suzuki, T., Shen, H., Akagi, K., Morse, H.C., Malley, J.D., Naiman, D.Q., Jenkins, N.A., Copeland, N.G., 2002. New genes involved in cancer identified by retroviral tagging. *Nat. Genet.* 32 (1), 166–174.
- Tamura, T., Ozato, K., 2002. ICSBP/IRF-8: its regulatory roles in the development of myeloid cells. *J. Interferon Cytokine Res.* 22 (1), 145–152.
- Tamura, T., Nagamura-Inoue, T., Shmeltzer, Z., Kuwata, T., Ozato, K., 2000. ICSBP directs bipotential myeloid progenitor cells to differentiate into mature macrophages. *Immunity* 13 (2), 155–165.
- Tanaka, N., Kawakami, T., Taniguchi, T., 1993. Recognition DNA sequences of interferon regulatory factor 1 (IRF-1) and IRF-2, regulators of cell growth and the interferon system. *Mol. Cell. Biol.* 13 (8), 4531–4538.
- Taniguchi, T., Ogasawara, K., Takaoka, A., Tanaka, N., 2001. IRF family of transcription factors as regulators of host defense. *Annu. Rev. Immunol.* 19, 623–655.
- Tsujimura, H., Nagamura-Inoue, T., Tamura, T., Ozato, K., 2002. IFN consensus sequence binding protein/IFN regulatory factor-8 guides bone marrow progenitor cells toward the macrophage lineage. *J. Immunol.* 169 (3), 1261–1269.
- Wang, I.M., Contursi, C., Masumi, A., Ma, X., Trinchieri, G., Ozato, K., 2000. An IFN-gamma-inducible transcription factor, IFN consensus sequence binding protein (ICSBP), stimulates IL-12 p40 expression in macrophages. *J. Immunol.* 165 (1), 271–279.
- Weisz, A., Marx, P., Sharf, R., Appella, E., Driggers, P.H., Ozato, K., Levi, B.Z., 1992. Human interferon consensus sequence binding protein is a negative regulator of enhancer elements common to interferon-inducible genes. *J. Biol. Chem.* 267 (35), 25589–25596.
- Weisz, A., Kirchhoff, S., Levi, B.Z., 1994. IFN consensus sequence binding protein (ICSBP) is a conditional repressor of IFN inducible promoters. *Int. Immunol.* 6 (8), 1125–1131.
- Yamada, Y., Matsushiro, H., Ogawa, M.S., Okamoto, K., Nakakuki, Y., Toyokuni, S., Fukumoto, M., Hiai, H., 1994. Genetic predisposition to pre-B lymphomas in SL/Kh strain mice. *Cancer Res* 54 (2), 403–407.
- Zhu, C., Rao, K., Xiong, H., Gagnidze, K., Li, F., Horvath, C., Plevy, S., 2003. Activation of the murine interleukin-12 p40 promoter by functional interactions between NFAT and ICSBP. *J. Biol. Chem.* 278 (41), 39372–39382.